Effects. Evidence now exists that intramolecular-exchange processes are quite frequent in the thermal decomposition of condensation polymers.[11] The thermal fragmentation of the polymer chains may occur through a ring–chain equilibration process which originates a series of cyclic oligomers, since the formation of cyclic compounds is favored at higher temperatures.

Of course, a kinetic control of the ring–chain exchange process takes place when the low molecular weight reaction products are quickly removed from the hot zone. Therefore, the ring concentrations observed in DPMS might differ from those at the equilibrium.[12]

DPMS data concerning *o*-, *m*-, and *p*-PPS indicate that intramolecular-exchange reactions predominate in the primary thermal decomposition processes of these polymers, causing the formation of cyclic oligomers.

Furthermore, a marked structural effect is observed in the distribution of the cyclic oligomers generated in the pyrolysis of *o*-, *m*-, and *p*-PPS.

In the case of *o*-PPS, in agreement with literature data,[13] only cyclic dimer is produced, while trimer and tetramer predominate in the case of the meta isomer over pentamer, hexamer, and heptamer. The cyclic distribution is different from those mentioned above in the case of *p*-PPS, where the cyclic pentamer is the most abundant product.

It appears therefore that the influence of polymer structure and conformation on the distribution of cyclic oligomers produced by the isomeric PPS I–III (Table I) is sensible.

In each case, the most abundant cyclic oligomer seems to correspond to the energetically most stable and conformationally preferred compound, indicating that the thermal decompostion process is controlled by structural and conformational factors.

The distribution of the cyclic oligomers formed in the polymerization reactions is also governed by structural and conformational factors. In fact, it is comparable with the distribution of the oligomers formed in the pyrolysis of *o*-, *m*-, and *p*-PPS.

Finally, it can be noted that spectra reported in Figure 4 allow us to differentiate by MS analysis the three isomeric PPS, which might prove a difficult task with other techniques.

Acknowledgment. The work was carried out under partial financial support from the Italian Ministry of Public Education and Consiglio Nazionale delle Ricerche.

Registry No. (*o*-$C_6H_4Br_2$)·(Na_2S) (copolymer), 102699-89-8; (*m*-$C_6H_4Br_2$)·(Na_2S) (copolymer), 102699-90-1; (*p*-$C_6H_4Br_2$)·(Na_2S) (copolymer), 57829-77-3; *o*-PPS, 82860-14-8; *m*-PPS, 32027-35-3; *p*-PPS, 25212-74-2.

References and Notes

(1) Zahn, H.; Gleitsman, G. B.; *Angew. Chem., Int. Ed. Engl.* **1963**, *2*, 410.
(2) Semylen, J. A. *Adv. Polym. Sci.* **1976**, *21*, 41.
(3) Goethals, E. J. *Adv. Polym. Sci.* **1977**, *23*, 103.
(4) Foti, S.; Maravigna, P.; Montaudo, G. *Macromolecules* **1982**, *15*, 883.
(5) Montaudo, G.; Puglisi, C.; Scamporrino, E.; Vitalini, D. *Macromolecules* **1986**, *19*, 870.
(6) Foti, S.; Montaudo, G.; In *Analysis of Polymer Systems*; Bark, L. S., Allen, N., S. Eds.; Applied Science: London, 1982; p 103 and references therein.
(7) Schulten, H. R.; Lattimer, R. P. *Mass Spectrom. Rev.* **1984**, *3*, 231.
(8) Montaudo, G. *Br. Polym. J.*, in press.
(9) Edmonds, J. T., Jr.; Hill, H. W., Jr. U.S. Patent 334129, 1967, *Chem. Abstr.* **1968**, *68*, 13598.
(10) Reents, W. D., Jr.; Kaplan, M. L. *Polymer* **1982**, *23*, 310.
(11) Montaudo, G.; Puglisi, C. In *Development in Polymer Degradation*; Grassie, N., Ed.; Applied Science: London, 1986; Vol 7 and references therein.
(12) Ballistreri, A.; Garozzo, D.; Montaudo, G. *Macromolecules* 1984, *17*, 1312.
(13) Hawkins, R. T. *Macromolecules* **1976**, *9*, 189.

Effects of Weak Linkages on the Thermal and Oxidative Degradation of Poly(methyl methacrylates)

Takashi Kashiwagi,* Atsushi Inaba,[†] and James E. Brown
National Bureau of Standards, Gaithersburg, Maryland 20899
Koichi Hatada, Tatsuki Kitayama, and Eiji Masuda
Department of Chemistry, Faculty of Engineering Science, Osaka University, Toyonaka, Japan. *Received March 6, 1986*

ABSTRACT: The thermal and oxidative degradation mechanisms of poly(methyl methacrylate) (PMMA) were studied in atmospheres of nitrogen and air by thermogravimetry using various specially polymerized samples. Thermal degradation of PMMA polymerized with a free radical method proceeds in three steps of weight loss: the least stable step is initiated by scissions of head-to-head linkages, the second step by scissions at the chain-end initiation from vinylidene ends, and the most stable step by random scission within the polymer chain. There are no significant differences seen in the thermal or oxidative degradation of PMMA polymerized with the free radical method between azobis(isobutyronitrile) and benzoyl peroxide as the initiators. Gas-phase oxygen traps radicals resulting from chain scissions at head-to-head linkages. No weight loss is observed from this step in air. Similarly, oxygen traps radicals generated by end initiation, but it is not as effective as for the case of head-to-head linkages. Possible mechanisms for end initiation and oxidative termination of radicals initiated from scission at the head-to-head linkages are discussed.

1. Introduction

If a vinyl polymer is polymerized by a free radical initiator, a termination reaction could occur through either disproportionation or combination reactions of two radical chains or by both in the absence of transfer agents. The disproportionation reactions yield an equal number of polymer chains with unsaturated end groups and saturated end groups. A polymer chain terminated by combination produces a head-to-head (H–H) linkage within the chain.

These abnormal linkages (unsaturated end group or a H–H linkage along the chain) might have significant effects on the thermal stability of the free radically polymerized

---

[†] Guest worker from National Research Institute for Pollution and Resources, Tsukuba, Japan.

0024-9297/86/2219-2160$01.50/0

Table I
Preparations of PMMA Samples

no.	init[a]	MMA, mol/L	MMA/Init, mol/mol	solvent	temp, °C	time, h	yield, %
A[b]	AIBN	6.40	10000	benzene	60	8	15.4
B[c]	AIBN	4.90	2000	benzene	60	20	79.0
C	AIBN	9.36	25	bulk	60	0.33	24.4
D	AIBN	9.36	400	bulk	60	1.0	18.0
E	AIBN	9.36	1000	bulk	60	1.0	7.2
F	BPO	9.36	25	bulk	60	0.5	17.3
G	BPO	0.91	100	benzene	60	2.5	14.9
H	DPHLi	0.85	100	THF	−78	2.0	75.7

[a] AIBN, azobis(isobutyronitrile); BPO, benzoyl peroxide; DPHLi, diphenylhexyllithium. [b,c] Polymerizations were carried out in the presence of *tert*-butyl mercaptan: A, 0.332 mol/L; B, 0.0245 mol/L.

polymer.[1] Although there have been many studies attempting to describe the effects of weak linkages on the thermal stability of polystyrene,[2-5] none of the possible abnormal structures considered (H–H, internal double bonds, branching) seem actually to be responsible for the thermal stability of polystyrene.[4-6] It has been suggested that poly(methyl methacrylate) (PMMA) chains having the unsaturated end group are less thermally stable than those with saturated end groups.[7] This suggestion has received wide support,[8-11] but no direct evidence for this proposal has been shown. For example, no direct evidence was given in these previous studies of the existence of unsaturated end groups (assumed to be the result of radical polymerization), of the structure of the unsaturated end groups (the location of the unsaturated bond), or of the quantity of chains having unsaturated end groups. There have been no previous studies describing the effects of H–H linkages on the thermal stability of PMMA. Recently, a more direct approach to determine the effects of unsaturated end groups and H–H linkages on the thermal stability of MMA oligomers were demonstrated to simulate the degradation of PMMA.[12] To further extend the evidence as to the effects of abnormal linkages on the thermal stability, the thermal degradation of various radically polymerized PMMAs was studied here.

Also important are the effects of gas-phase oxygen on the abnormal linkages. The reported effects of oxygen on the thermal stability of PMMA are not self-consistent. An early study[13] reported that degradation of PMMA was observed in air at 200 °C but not observed in nitrogen. Another study[14] reported that oxygen has a strong inhibiting effect on the degradation of powdered PMMA but that it accelerates the degradation of bulk specimens. Our previus results[15,16] show a small increase in thermal stability in the presence of oxygen below 200 °C and a significant decrease in stability above 230 °C for degradation of a commercial PMMA. It appears that gas-phase oxygen displays a dual character in its effects on the degradation of PMMA.

In this study, the effects of the abnormal linkages on thermal stability of PMMA in a nitrogen atmosphere are studied first and then the effects of gas-phase oxygen on each abnormal linkage are reported.

2. Preparation and Characterization of PMMAs

Methyl methacrylate (MMA) was obtained commercially and purified by fractional distillation under nitrogen. The distillate was dried over calcium dihydride and then vacuum distilled. Benzene was distilled over sodium under nitrogen pressure, and the distillate was dried with butyllithium and redistilled under high vacuum. Tetrahydrofuran (THF) was refluxed over lithium aluminum hydride and then distilled under high vacuum.

Polymerization of MMA was carried out in a sealed glass ampule after being thoroughly degassed and filled with nitrogen. The reaction mixture was poured into a large amount of methanol to precipitate the polymer formed. The polymer was reprecipitated from benzene or chloroform into methanol. The precipitate was collected by filtration, washed several times with methanol, and dried in vacuo at 60 °C. Seven PMMA samples were prepared with azobis(isobutyronitrile) (AIBN) or benzoyl peroxide (BPO) in bulk or in benzene at 60 °C and one with diphenylhexyllithium (DPHLi) in THF at −78 °C. The polymerization conditions and the polymer yields for these samples are shown in Table I.

Table II
Molecular Weights and Tacticities of PMMA Samples

no.	tacticity, % I	H	S	M_n	M_w/M_n[a]
A	7.8	32.0	60.2	10 200[a]	1.46
B	5.1	34.8	60.2	17 400[a]	1.88
C	7.5	33.1	59.4	44 600[b]	1.67
D	6.4	33.2	60.4	176 000[a]	2.51
E	6.3	33.3	60.4	320 000[a]	4.89
F	5.1	32.7	62.2	54 800[a]	1.78
G	5.7	33.7	60.6	43 400[a]	1.70
H	2.6	14.4	83.0	12 900[a]	1.35

[a] Determined by GPC. [b] Determined by VPO.

The amounts of olefinic protons and BPO fragments at the chain ends of PMMAs were determined from the ^{1}H NMR spectra of the polymers taken in deuterated chloroform on JNM-FX100[26] (100 MHz), JNM-GX270 (270 MHz), and JNM-GX400 (400 MHz) Fourier transform NMR spectrometers (JEOL) at 55 °C with tetramethylsilane as an internal standard. The analytical procedure was described in a previous paper.[17] NMR spectroscopy has been adopted successfully for the analysis of the terminal structure of polymers.[17-20]

The molecular weights of the polymers were measured by using a Hitachi 117 vapor pressure osmometer in toluene at 60 °C or a Jasco FLC-A10 GPC chromatograph with a Shodex GPC column A-80M (50 cm × 2) with maximum porosity of 5×10^7 with tetrahydrofuran as a solvent. The GPC chromatograph was calibrated against standard polystyrene samples. The results of the measurements are summarized in Table II.

3. Thermogravimetry

The polymer degradation characteristics were determined by thermogravimetry (TG) using a Mettler TA2000 thermoanalyzer. When nitrogen was used as a test gas, the furnace and the TG system dead volume were subjected to two repeated cycles of evacuation and filling with nitrogen to atmospheric pressure. The maximum oxygen concentration in the furnace was 50 ppm. A heating rate of 2 °C/min was used in this study to make sure that mass transport processes of oxygen and degradation products through the sample did not affect the experimental results.[15,16] The samples were fine powders and were spread thinly over the bottom of a prebaked aluminum pan about 5.5 mm in diameter. The weight of the samples ranged from 4 to 5 mg. The sample pan was set at the center of the sample support over the thermocouple, whose output was used to control the temperature of the furnace.

The weight of the sample, its temperature, and the time were simultaneously recorded by a computer. At first, a base-line run without a sample was conducted and then an identical run with a sample was repeated. The actual weight of the sample was calculated from the difference between the sample run and the

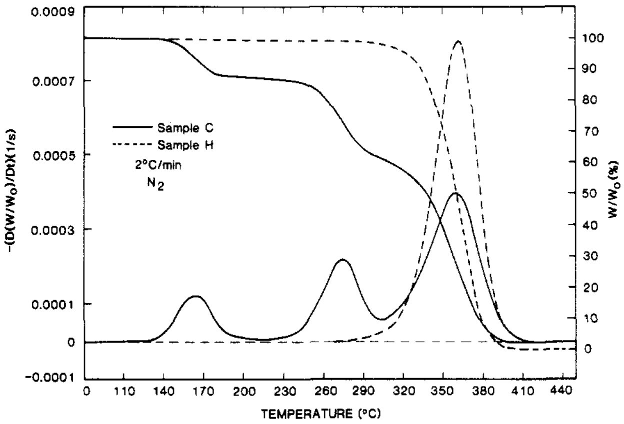

Figure 1. Effects of the polymerization method on DTG curves for samples degrading in nitrogen: sample C (radically polymerized) and H (anionically polymerized).

base-line run. This procedure removed the artificial change in the weight caused by buoyancy generated by heating the furnace.

The molecular weights of the residues halted during the thermal gravimetry were measured by using a Waters Associates Model ALC/GPC-150C gel permeation chromatograph equipped with a column set consisting of Waters μStyragel 10^3, 10^4, 10^5, 10^6, and 10^2 Å with tetrahydrofuran as a solvent. The calibrated molecular weight range of the column set was from 8×10^2 to 7.5×10^6 against standard PS and PMMA samples.

4. Results and Discussion

4.1. Thermal Degradation. In this section, TG results for a sample degraded in a nitrogen atmosphere are discussed.

4.1.1. Radically Polymerized Sample vs. Anionically Polymerized Sample. A comparison of TG results between sample C (radically polymerized) and sample H (anionically polymerized) is shown in Figure 1. The derivative thermogravimetry (DTG) results were obtained by taking the time derivative, $d(W/W_0)/dt$, of the ratio of the sample weight, W, to the initial sample weight, W_0. The DTG curve of sample H shows one sharp peak around 360 °C. On the other hand, the DTG curve of sample C shows three distinct peaks, around 165, 270, and 360 °C at a heating rate of 2 °C/min. The peak height increases with increasing temperature. The first peak around 165 °C became very small when there was a small amount of oxygen in the furnace (~0.1%). The oxygen sensitivity of this peak will be discussed later. Since the third peak (around 360 °C) appears to correspond to the single peak of the anionically polymerized sample H, which contains no irregular structures such as H–H linkages or unsaturated end groups, it is reasonable to infer that this peak is caused by random scission initiation. Then, the question remains as to what causes the other two peaks.

With the use of various oligomers as model compounds,[12] it was reported that the least stable linkage in the oligomers was the H–H linkage at around 195 °C (for a TG heating rate of 20 °C/min). The second most unstable linkage (at about 255 °C) was attributed to unsaturated vinylidene ends. The most stable linkage was observed with a saturated oligomer that started to degrade around 300 °C. Our results here for sample C appear to agree qualitatively with the above-described three peaks. Since higher heating rates (20 °C/min in the previous study[12] vs. 2 °C/min of this work) tend to increase the peak temperature of the degradation, it is apparent that the first peak corresponds to depolymerization initiated from the weak H–H linkages and the second peak to end-initiated depolymerization from the unsaturated vinyl ends. Further confirmation of what causes the two peaks at low temperatures is one of the major objectives of this study.

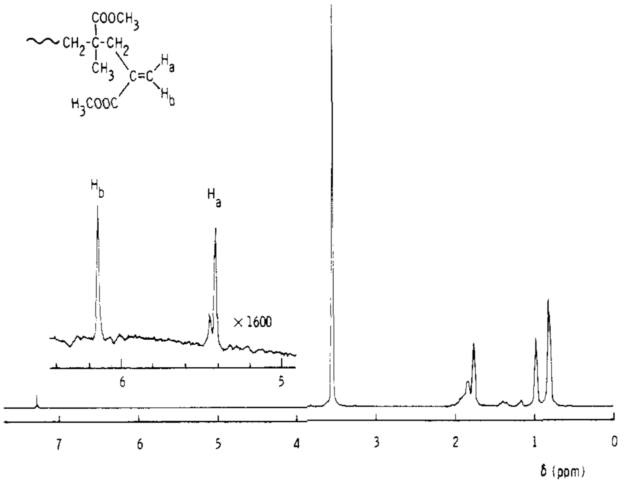

Figure 2. ^1H NMR spectrum of sample C ($CDCl_3$, 55 °C, 270 MHz).

Table III
Fraction of Irregular Structures in a Radically Polymerized PMMA Molecule

no.	$-CH_2-C(=CH_2)-COOCH_3$	$-C(CH_3)(COOCH_3)-C(CH_3)(COOCH_3)-$
A	~0	
B	0.034	
C	0.36	0.28

4.1.2. Olefinic End Group. Three samples, A, B, and C, were prepared so as to have different amounts of unsaturated groups at the polymer ends; this was achieved by the use of a chain-transfer agent for samples A and B. Hatada et al.[17] demonstrated by ^{1}- NMR spectroscopy that the termination by disproportionation in the radical polymerization of MMA occurred mostly through route a of the following equation and not through route b.

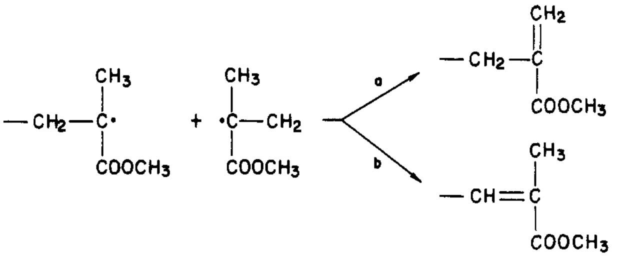

A 270-MHz ^1H NMR spectrum of sample C is shown in Figure 2, which shows no trace of monomers. The peaks at 5.4 and 6.14 ppm have been assigned to the methylene protons of the vinylidene group, which is formed through route a. The fraction of polymer molecules that contains the vinylidene group at the chain end can be determined from these methylene proton signals since the effect of a chain-transfer reaction to MMA monomer can be neglected.[17] Intensity measurements of these signals showed that 36% of the polymer molecules contained a vinylidene double bond at the chain ends; that is, 72% of the molecules formed through a disproportionation reaction. Then the residual 28% of the molecules should be formed through a combination reaction and contain an H–H linkage in the chain (Table III).

When the polymerizations were carried out in the presence of *tert*-butyl mercaptan, the amount of vinylidene chain ends decreased greatly as shown in Table III (sam-

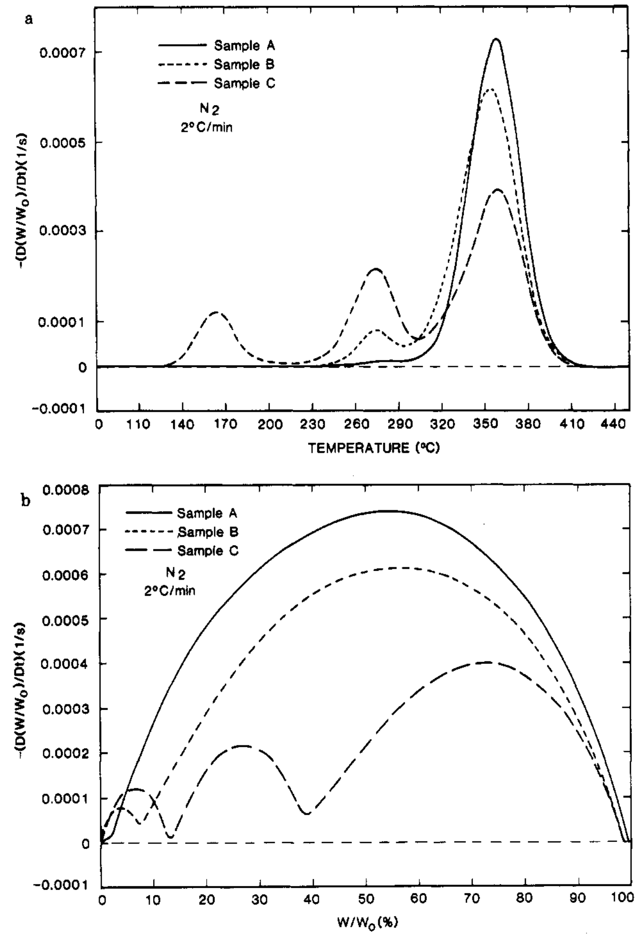

Figure 3. (a) Effects of amount of vinylidene ends on DTG curves for samples degrading in nitrogen, samples A (~0.0), B (~0.034), and C (0.36). (b) Effects of amount of vinylidene ends on relationships between $d(W/W_0)/dt$ vs. W/W_0 in nitrogen with samples A, B, and C.

ples A and B). In the presence of mercaptan almost all the polymer molecules formed contain one fragment of chain-transfer agent.[17] This means that samples A and B contain very few H–H linkages.

The DTG results for the three samples are shown in Figure 3a. Samples A and B do not show any detectable weight loss from least stable linkages (around 165 °C), and hardly any weight loss as shown by a second peak appears for sample A. For all three samples, the most stable linkages generate the largest peak corresponding to degradation caused by random scission initiated within the polymer chains. The same results are plotted against the normalized weight loss, W/W_0, shown in Figure 3b. This figure gives an idea as to how much of the sample weight loss is caused by each peak shown in Figure 3a. The curve for sample A, having no unsaturation detected by NMR, shows that the mass loss caused by the second peak is at most 2% of the initial weight of the sample. This is about 7% for sample B, which has terminal double bonds at 3.5% of the chains. For sample C with 28% H–H linkages and 36% terminal double bonds of polymer chains, these are about 13% and 25% for the first and second peaks, respectively.

If each polymer chain unzips without any termination reactions to halt it, the mass loss caused by an H–H linkage or by an unsaturated vinylidene end could be estimated if the structure of the sample was well characterized. It is expected that a combination reaction during the termination of the polymerization process produces an average polymer chain twice as long as those terminated by disproportionation. The ratio of all linkages in chains that somewhere have a H–H linkage compared to the total number of linkages in the sample can be expressed as $(0.28 \times 2)x_0/(0.36 + 0.36 + 0.28 \times 2)x_0$, where x_0 is number-average initial degree of polymerization of the sample. Therefore, the normalized mass losses from sample C should be at most 44% due to the H–H linkages. This discrepancy is due to the assumption of complete unzipping of each polymer chain during degradation. There are four possible paths for polymer radicals created from chain scission at the H–H linkages: (1) complete unzipping; (2) termination during the depolymerization process; (3) disproportionation termination of the radicals initiated by the chain scission at the H–H linkages, due to cage effects under expected high viscosity of the sample at this temperature range (~165 °C), as

Table IV
Molecular Weight of Residue/Initial Molecular Weight of the Sample ($\bar{M}_n/\bar{M}_{n0}$)[a]

	sample C	sample D
degradation in nitrogen halted at 200 °C	0.97	0.90
degradation in nitrogen halted at 280 °C	0.79	0.68
degradation in air halted at 200 °C	0.90	

[a] At a heating rate of 2 °C/min.

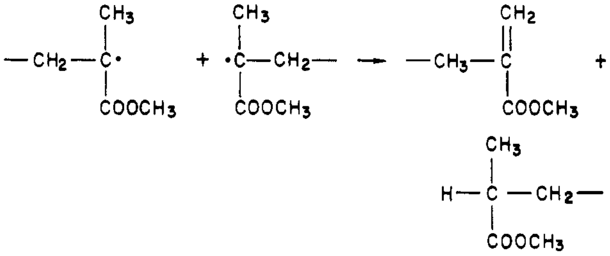

$$-CH_2-\underset{COOCH_3}{\overset{CH_3}{C}}\cdot + \cdot\underset{COOCH_3}{\overset{CH_3}{C}}-CH_2- \longrightarrow -CH_3-\underset{COOCH_3}{\overset{CH_2}{\overset{\|}{C}}} + H-\underset{COOCH_3}{\overset{CH_3}{C}}-CH_2- \qquad (1)$$

(as described in the beginning of this section, hydrogen is abstracted from methyl instead of methylene, although it is primary hydrogen); and (4) polymerization of monomers generated from unzipping with polymer radicals because the ceiling temperature (197 °C[21]) is near or above the temperature range in which the weight loss occurrs from the chain scission at the H–H linkages. If all chains that have the H–H linkages are terminated by disproportionation immediately after the chain scission at the H–H linkages described by eq 1 (28% of the total number of chains), the number-average molecular weight, $\bar{M}_n$, should be about 78% of the initial number-average molecular weight, $\bar{M}_{n0}$. If all chains with the H–H linkages are unzipped, again $\bar{M}_n$ becomes 78% of $\bar{M}_{n0}$ (this is equal to the molecular weight of the original polymer chains without any H–H linkages). If the depolymerization is halted by termination during the unzipping process, $\bar{M}_n$ decreases below 78% of $\bar{M}_{n0}$. With the polymerization (as listed in the fourth possible path), $\bar{M}_n$ could be larger than 78% of $\bar{M}_{n0}$.

The measured value of $\bar{M}_n$ of the sample residue whose heating in nitrogen atmosphere at 2 °C/min was halted at 200 °C is about 97% of $\bar{M}_{n0}$ as listed in table IV. A small decrease in $\bar{M}_n$ and about one-third of the maximum possible weight loss ratio (13% instead of 44%) by chain scissions at the H–H linkages indicates that unzipping, termination of the radicals described by eq 1, and the polymerization (the fourth path) would occur simultaneously and compete. It is not clear at present what combination of these processes produces the observed weight loss ratio and molecular weight reduction. Since the average zip length (the average number of monomer units successively released by depolymerization along the length of a polymer chain) is expected to be far above 1000 at this temperature range (~165 °C),[15] it is expected that the probability for termination to occur during the depolymerization process is very small.

Additional strong evidence to support the hypothesis that the least stable peak shown in Figure 3a is caused by chain scissions at the H–H linkages is that no detectable weight loss is observed around 165 °C for samples A and B. This is consistent with the observation that samples A and B contain very few H–H linkages, as described in the beginning of this section. Also, the temperature for the first peak shown in Figure 3a appears to agree with that seen in the degradation of the model compound (an oligomer), simulating the H–H linkage of PMMA.[12] Furthermore, the bond dissociation energy of the H–H linkage is estimated to be about 84 kJ/mol (20 kcal/mol) less than that of C–C backbone bond, E_{cc}, due to a large steric hindrance and inductive effect of vicinal ester groups.[22] Therefore, weight loss initiated by chain scissions at the H–H linkages should occur at the lowest temperatures compared with those due to end initiation (roughly 42–50 kJ/mol less than E_{cc} described later) or random scission. Therefore, the first weight loss peak shown in Figure 3a is considered to be due to chain scissions at the H–H linkages.

The normalized weight loss of the second stable peak (around 270 °C) shown in Figure 3 decreased in the order of samples C > B > A, which is the same as the decreasing order of the measured fraction of the polymer chains with the unsaturated double bonds at the chain ends. Therefore, it is reasonable to consider that the second peak shown in Figure 3a is initiated from the unsaturated double bonds at the chain ends. With the data listed in Table III, the normalized mass losses from sample C should be at most 28% due to unzipping initiated from the unsaturated double bonds at the chain ends. However, the experimentally determined normalized mass losses are about 25% as shown in Figure 3b. Although these two values are close to each other, this does not necessarily mean that complete unzipping occurs from end initiation. As discussed earlier, only 13% of the weight loss occurred due to chain scissions at H–H linkages instead of the maximum 44% inferred from assuming complete unzipping. It is possible that some of the polymer chains, which stay in the sample, might have unsaturated double bonds at the chain ends as a result of the above-described, complex processes consisting of termination and polymerization following chain scissions at H–H linkages. Therefore, there might be more chains having unsaturated double bonds at the chain ends than the initial 36%. Also, chains with newly formed unsaturated double bonds would be longer than those initially having an unsaturated double bond because the reduction in $\bar{M}_n$ is so small after a chain scission at a H–H linkage. Since the average zip length decreases with increasing temperature,[15] termination becomes more probable in this temperature range (~270 °C) than for the first peak (~165 °C). The more frequent occurrence of termination during the depolymerization process is confirmed by the measured number-average molecular weight of a sample residue obtained from heating at 2 °C/min to 280 °C. The value of $\bar{M}_n$ of the sample residue decreased significantly (as listed in Table IV), implying that termination reactions stopped the unzipping process initiated from the chain ends.

As discussed above, the location of the unsaturated double bond at the chain end is clarified, but it is not clear how the end initiation begins. There are at least two possibilities: (1) β scission, and (2) an ene reaction. Since a carbon–carbon bond β to the double bond is roughly 42–50 kJ/mol weaker than a neighboring saturated carbon–carbon bond, the scission could occur as follows:

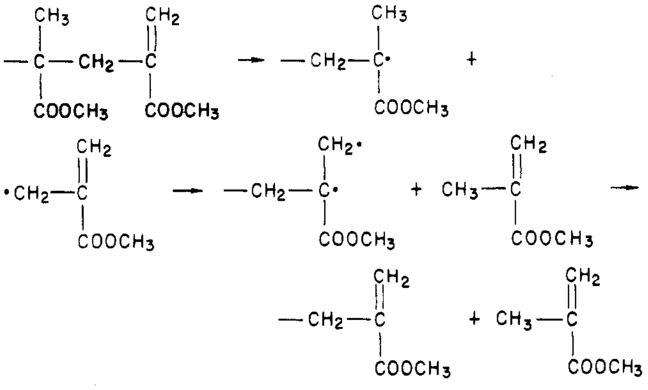

The abstraction of hydrogen from methyl instead of methylene is consistent with the obervation of a vinylidene group instead of a trisubstituted olefinic double bond at the chain end as discussed earlier (if hydrogen is abstracted from methylene, a trisubstituted olefinic double bond is formed at the chain end).

If the end initiation occurs due to the ene reaction, it would be

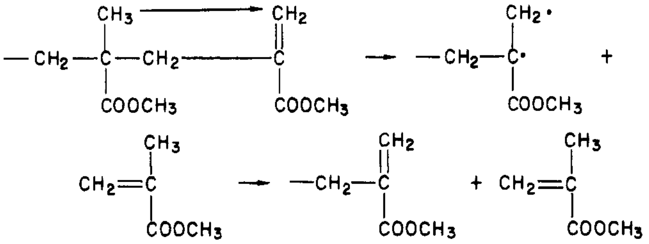

The importance of the ene reaction was demonstrated for end initiation of polyisobutylene.[23] There might be other paths for the end initiation. If one of the above proposed reaction mechanisms is the correct one, the depolymerization from the end initiation is the continuation of the end initiation step (each step generates a new vinylidene group at the chain end). Further detailed studies are needed to clarify the end initiation mechanism.

4.1.3. Effects of Initial Molecular Weight, $\bar{M}_{n0}$. The effects of initial molecular weight on degradation characteristics were examined with samples C, D, and E. These samples were polymerized in bulk at the same temperature (60 °C) with the same initiator (AIBN). It is therefore expected that the fractions of polymer chains with H–H linkages and with vinylidene ends are the same for the three samples. Their DTG results are shown in Figure 4a against temperature and in Figure 4b against normalized weight loss. All three samples show three peaks corresponding to the above-discussed initiation mechanisms for degradation, i.e., initial scission at H–H linkages, vinylidene groups, and random bonds in the polymer chain, but sample E has four peaks. The initial molecular weight distribution of sample E is bimodal, and it has a large polydispersity of 4.89. It appears that some other unstable linkages were formed in the polymer chains during its polymerization, which generated the additional peak at around 200 °C. With an increase in initial molecular weight, the heights of the first and second peaks decrease, corresponding to a lower fraction of weight loss by these peaks (the first peak for sample E is an exception). For example, the fraction of weight loss decreases from approximately 13% to 3% for the first peak between sample C and D. For the second peak, it decreased from ap-

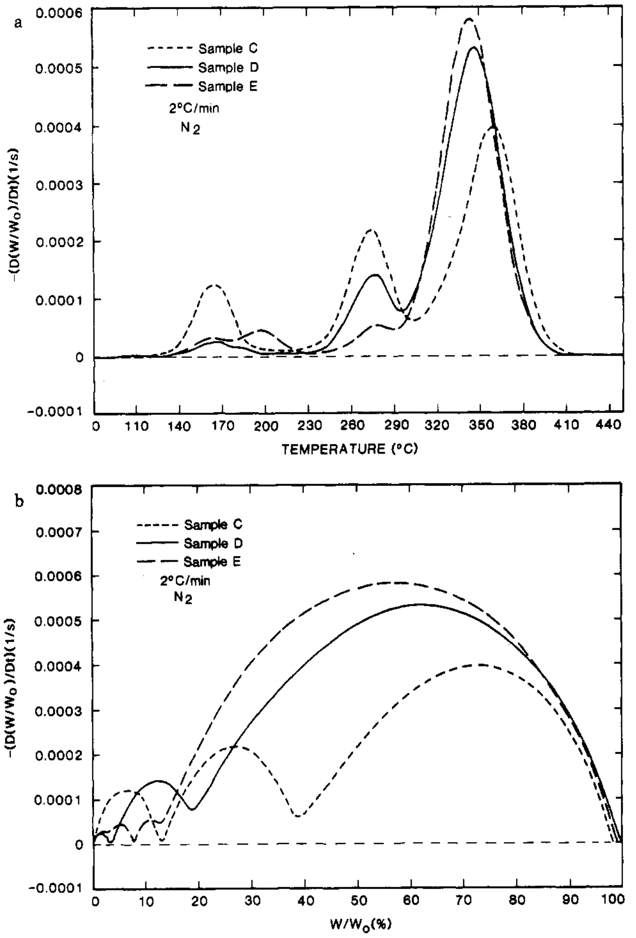

Figure 4. (a) Effects of $\bar{M}_{n0}$ on DTG curves for samples degrading in nitrogen, samples C ($\bar{M}_{n0}$ = 44600), D (176000), and E (320000). (b) Effects of $\bar{M}_{n0}$ on relationships between $d(W/W_0)/dt$ vs. W/W_0 in nitrogen with samples C, D, and E.

proximately 25% for sample C to 16% for sample D and further to 5% for sample E. The fraction of the number of polymer chains with each of the above-described weak linkages, N_w/N_0, remains at the same value with an increase in the initial molecular weight of the sample as long as the samples are polymerized at the same temperature and with the same initiator assuming there is no abnormal polymerization. If $\bar{M}_{n0}$ is much less than the average zip length, Z, the fraction of weight loss from each of these weak linkages is proportional to N_w/N_0 and does not change with an increase in $\bar{M}_{n0}$. However, if $\bar{M}_{n0}$ is close to or less than Z, the fraction of weight loss from each of these weak linkages is proportional to $(N_wZ)/(N_0\bar{M}_{n0}/\mathrm{MW})$, where MW is the molecular weight of a monomer. Therefore, the fraction of weight loss from each of these weak linkages decreases with an increase in $\bar{M}_{n0}$. In this range of $\bar{M}_{n0}$, the probability that termination occurs increases with an increase in $\bar{M}_{n0}$. This is confirmed by the fact that the ratios of $\bar{M}_n/\bar{M}_{n0}$ of the sample residues after the first peak and the second peak decrease more with an increase in $\bar{M}_{n0}$ as listed in Table IV.

It is interesting to note that the peak height for the random scission step (the most stable peak in Figure 4a) increases with an increase in $\bar{M}_{n0}$. This means that the partially degraded polymer chains remaining, whose degradation was initiated from the weak linkages, do not have any more of these weak linkages and degrade subsequently only by random scission. Another important point is that the third peak (caused by random scission) appears at lower temperature with an increase in initial molecular weight. A similar trend is also observed with anionically polymerized PMMA.[24] A further detailed discussion of effects of initial molecular weight on degradation will be reported in a future paper.

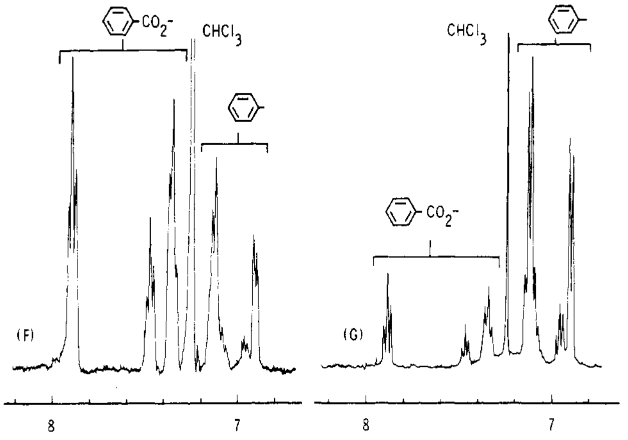

Figure 5. ^{1}H NMR spectra of PMMAs prepared with BPO in bulk (sample F) and in benzene (sample G) at 60 °C ($CDCl_3$, 55 °C, 400 MHz).

4.1.4. Effects of Initiator. It was speculated that AIBN-initiated vinyl polymers are usually more stable than those prepared with peroxide initiators.[1] Also with benzoyl peroxide (BPO) as the initiator, benzylic methylene generated from the phenyl radical at the beginning of the polymer chain was asserted to be more susceptible to a variety of hydrogen abstraction and oxidation reactions than benzoyloxy-initiated molecules. To examine these ideas, the thermal stability of sample C (AIBN initiated) and of samples F and G (BPO initiated) was studied. These samples have similar initial molecular weights (listed in Table II). The difference between sample F and G is the difference in the ratio of benzoyloxy-initiated polymer chain heads to phenyl-initiated polymer chain heads. This ratio was determined from the ^{1}H NMR spectra which show the signals due to phenyl and benzoyloxy groups separately.[17] The aromatic proton regions of the 400-MHz ^{1}H NMR spectra of samples F and G are shown in Figure 5. The peak assignments were made according to a previous paper[17] and are indicated in the figure. Intensity measurements indicated that the ratios of benzoyloxy group to phenyl group at the beginning of the chain were 72/28 and 21/79 for the samples F and G, respectively. The ratios agree roughly with those (91/9 and 21/79)[25] obtained with ^{14}C-labeled BPO for the polymers prepared in bulk and at the monomer concentration of 0.91 mol/L, respectively.

If the previous speculation is correct, sample C should be the most stable, followed by sample F; the least stable sample should be sample G. The DTG results for the three samples are shown in Figure 6. There are the three peaks for samples F and G at about the same temperatures as those for sample C. The heights of the three peaks are about the same for all three samples. Therefore, the overall thermal stability of PMMA prepared with AIBN and BPO is basically the same; also, the thermal stability of phenyl-initiated PMMA is equal to that of benzoyloxy-initiated PMMA except for minor, secondary effects on the end-initiated degradation peak (second peak).

4.2. Thermal Oxidative Degradation. An important question is how gas-phase oxygen modifies the thermal degradation of radically polymerized PMMA. It is especially important to find how gas-phase oxygen affects the degradation initiated by H–H linkages and by end initiation. The following experiments were conducted to find how oxygen affects the low-temperature degradation ob-

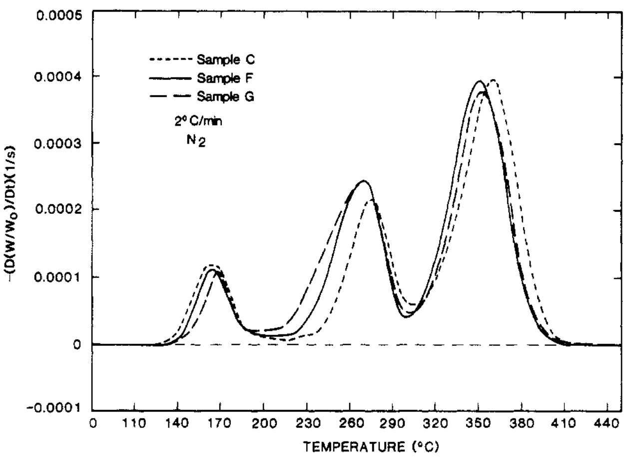

Figure 6. Effects of initiator on DTG curves for samples degrading in nitrogen, samples C (AIBN), F (BPO), and G (BPO).

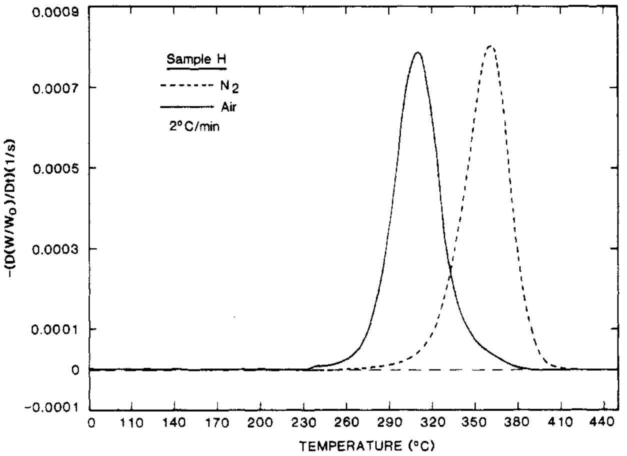

Figure 7. Effects of oxygen on DTG curves for sample H (anionically polymerized).

served in a nitrogen atmosphere.

DTG results for anionically polymerized sample H degraded in air are compared with those degraded in nitrogen in Figure 7. Both results show only one peak. However, sample H degrades in air at substantially lower temperatures than in nitrogen; the difference in temperature of the DTG peak between the two atmospheres is about 50–60 °C. Although the detailed mechanism of the effects of oxygen on the degradation is not clearly understood at present, gas-phase oxygen definitely enhances the degradation of this anionically polymerized PMMA. However, the effects of gas-phase oxygen on the degradation of radically polymerized PMMA are much more complex than those on anionically polymerized PMMA as shown in Figure 8 for sample C.

With sample C, the first peak caused by the H–H linkage degraded in a nitrogen atmosphere completely disappears when the sample is degraded in air. The second peak caused by end initiation in a nitrogen atmosphere is slightly stabilized (shifted toward high temperatures), but Figure 8 indicates that there is definitely some degradation caused by end initiation in the presence of air. The third peak caused by random scission in a nitrogen atmosphere is hardly present in air. However, a new major peak appears at around 300 °C in air between the second and the third peaks observed in a nitrogen atmosphere. Therefore, gas-phase oxygen plays a dual role in the degradation of radically polymerized PMMA by suppressing its degradation caused by the weak linkages at low temperatures and by enhancing its degradation at high temperatures.

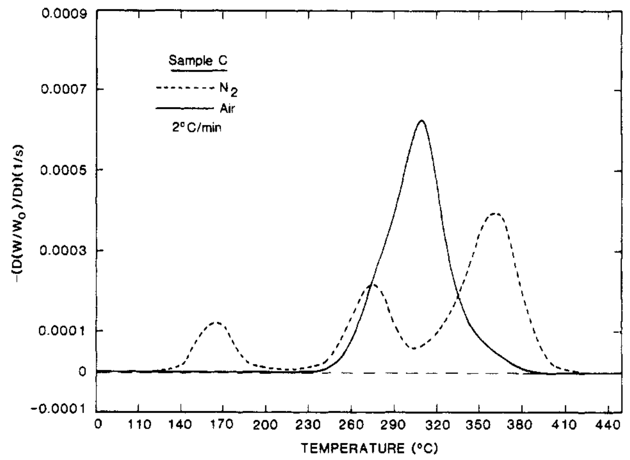

Figure 8. Effects of oxygen on DTG curves for sample C (radically polymerized).

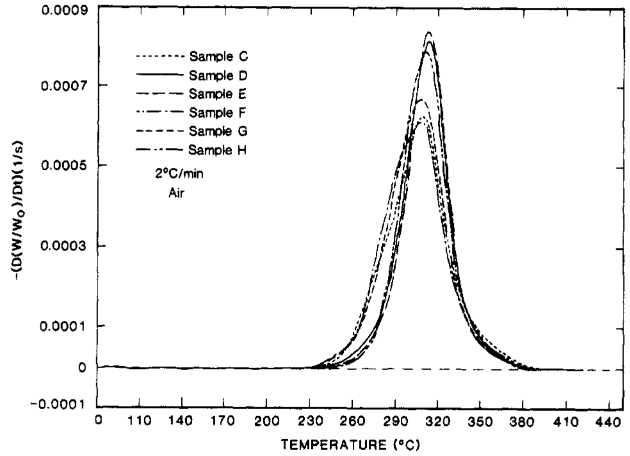

Figure 9. Effects of polymerization, initiator and $\bar{M}_{n0}$, method on DTG curves for samples degrading in air, samples C (radical, AIBN, 44 600), D (radical, AIBN, 176 000), E (radical, AIBN, 320 000), F (radical, BPO, 54 800), G (radical, BPO, 43 400) and H (anionic, DPHLi, 12 900).

The new major peak in air occurs in the temperature range similar to that for anionically polymerized PMMA degraded in air. Apparently then, the weight loss of PMMA degrading in air is not as sensitive to differences in PMMA structure (initial molecular weight and the polymerization method) as it is in a nitrogen atmosphere. This is demonstrated in Figure 9. All six samples involving different initial molecular weights, initiators and polymerization methods show basically the same peak when they degrade in air. The only noticeable difference is due to the degradation contribution from end initiation when the sample has a significant amount of vinylidene groups at chain ends. The degradation contribution from end initiation can be seen at the lower temperature side of the peaks in Figure 9. As discussed in section 4.1.3, the fraction of weight loss from end initiation becomes small for samples D and E with large values of $\bar{M}_{n0}$, although the number of polymer chains with a vinylidene group at the chain end for samples D and E should be close to that for sample C. Therefore, samples D, E, and H show little broadening at the lower temperature side of the peak.

At first, sample C was heated in air to 200 °C at a heating rate of 2 °C/min. There was no detectable weight loss of the sample during this heating period. After the sample was cooled to ambient temperature, the sample was reheated in a nitrogen atmosphere to 440 °C at a heating rate of 2 °C/min. The DTG results of this experiment in nitrogen are shown in Figure 10. Similarly to degradation

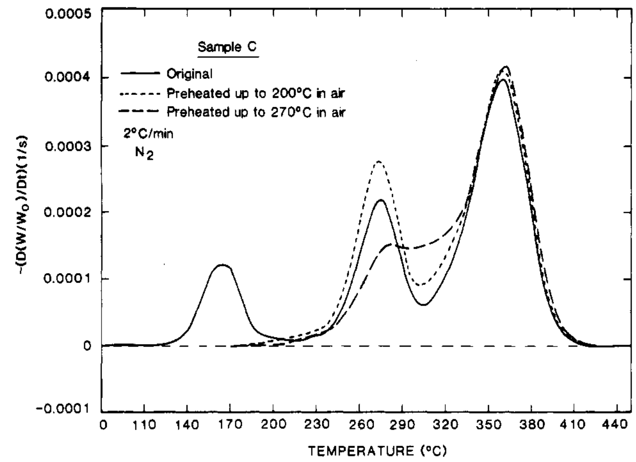

Figure 10. Effects of preheating temperature in air on DTG curves for sample C degrading in nitrogen.

of the sample in air, there is no peak around 160–170 °C even though the preheated sample was degraded in a nitrogen atmosphere. This indicates that the sample preheated in air does not have any H–H linkages. It appears that, when radicals are formed after the chain scission of these H–H linkages, oxygen traps the radicals and terminates them. This process is confirmed by a reduction in molecular weight of the sample residue heated to 200 °C in air at a heating rate of 2 °C/min. The measured value of $\bar{M}_n/\bar{M}_{n0}$ for sample C is 0.90, listed in Table IV, which is a little higher than 0.78 calculated by assuming that the radicals generated by chain scissions at H–H linkages are trapped by oxygen and terminate by disproportionation to form two polymer molecules before they depolymerize. Higher values of $\bar{M}_n$ indicate that polymer radicals with oxygen attached would terminate by a combination reaction to form polymer peroxides with almost the same chain length as the polymer chain. It appears that a combination of these two termination reactions, described below, (1) disproportionation, and (2) combination after radicals react with oxygen, can explain why there is no detectable weight loss and some reduction in $\bar{M}_n$ caused by chain scissions at H–H linkages for the sample heated in air. This also agrees with why there is no detectable weight loss caused by chain scissions at H–H linkages for the sample heated in air.

Scheme I shows a possible chemical reaction scheme to explain the role of oxygen on degradation initiated at H–H linkages that is inferred from the above observation.

Disproportionation of radicals I is very difficult because there are no α hydrogens. Step 2 is based on 1,5 hydrogen transfer and combination. There may be another possible reaction associated with oxygen trapping.

Other important features shown in Figure 10 are that (1) the second peak of the preheated sample is larger than that of the original unheated sample; (2) the valley between the second peak and third peak for the preheated sample is less deep than for the original unheated sample (this temperature range corresponds to that for the major peak of degradation in air as shown in Figures 8 and 9); (3) the third peak of the preheated sample does not change at all from that of the original unheated sample. These results indicate that, after radicals generated by chain scissions at H–H linkages are trapped by oxygen, a part of them form olefinic ends and the rest form less stable polymer chains with peroxides than those originally having no weak linkages.

The other DTG curve shown in Figure 10 was obtained by a similar experiment except that sample C was preheated to 270 °C in air instead of to 200 °C as in the previous experiment. This caused a weight loss of about 10%. Comparison of this DTG curve (270 °C) to the other two in Figure 10 implies that gas-phase oxygen traps some of the radicals originating from vinylidene ends. However, this trapping is not as effective as that for the H–H linkages. It is speculated here that degradation initiated from vinylidene ends might follow the two paths described in section 4.1.2 simultaneously, one by the β scission path and the other by the ene reaction path. Thus, the oxygen-trapping effect is mainly from the β scission path. There might be another reason. Since the temperature range in which end initiation occurs is higher than that for chain scissions at H–H linkages, the rate of depropagation for the second peak is much faster than that for the first peak. Therefore, radical trapping by oxygen at this temperature range must compete with relatively fast depropagation so that it is not as effective as that for the lower temperature range.

Scheme I

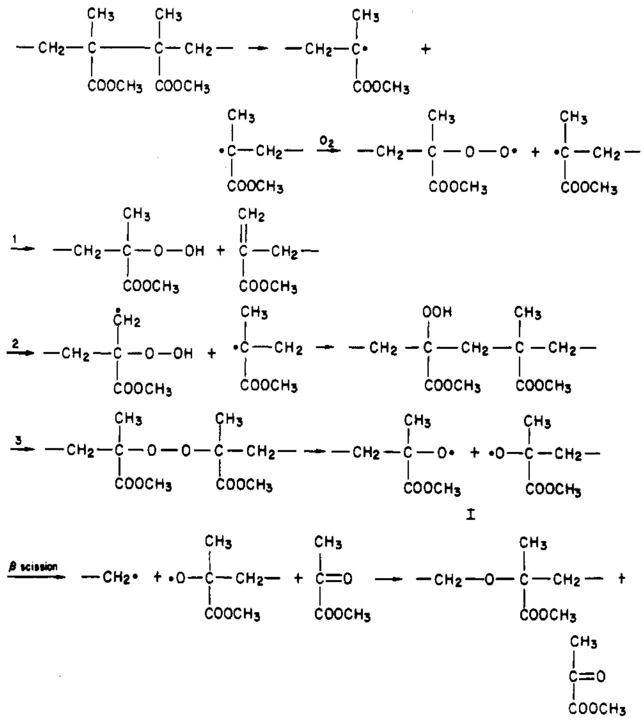

The major peak in Figures 8 and 9 for degradation in air is due to mainly two reactions. One of them is due to degradation of partially oxidized groups, such as peroxides as discussed above. These polymer chains are formed by oxygen trapping of the radicals that are generated from the weak linkages. The other is oxygen attack to the radicals that are generated by random scission within the polymer chain. As shown in Figures 7 and 8, the beginning of the random scission peak (third peak) appears to overlap with the major peak for degradation in air. Then, it is expected that radicals formed by random scission with the chain react with oxygen to form ROO·, which subsequently abstracts hydrogen to form ROOH. The dissociation of ROOH forms RO· and very reactive ·OH. Thus, the ROOH could generate two radicals that subsequently attack other polymer chains, yielding rapid degradation.

5. Conclusions

1. The degradation of PMMA, polymerized by a free radcal method, in a nitrogen atmosphere may be initiated by any one of three reactions. The least stable reaction is chain scissions at H–H linkages. The second reaction

is chain end initiation from vinylidene chain ends. The most stable reaction is random scission initiation within the polymer chains. At a heating rate of 2 °C/min, the peak temperature of each reaction in the DTG curve is about 165, 270, and 360 °C, respectively.

2. Chain-transfer agents used in the polymerization process apparently significantly reduce the number of H–H linkages and vinylidene ends and thereby stabilize radically polymerized PMMA.

3. The different initiators used in this study, AIBN and BPO, do not produce significant differences in the thermal and oxidative degradation of PMMA. Also, phenyl radical initiated polymer chains and benzoyloxy radical initiated polymer prepared with BPO do not cause any significant difference in the thermal and oxidative degradation of PMMA.

4. Gas-phase oxygen very effectively traps radicals originating from chain scissions at the H–H linkages. Similarly, oxygen also traps some of radicals generated by end initiation. However, this trapping by oxygen is not as effective as that for the H–H linkage.

Acknowledgment. We thank Dr. Wing Tsang at NBS for his valuable discussions and suggestions regarding degradation chemistry.

Registry No. PMMA (homopolymer), 9011-14-7.

References and Notes

(1) Solomon, D. H. *J. Macromol. Sci., Chem.* **1982**, *A17*(2), 337.
(2) Grassie, N.; Kerr, W. W. *Trans. Faraday Soc.* **1957**, *53*, 234.
(3) Richards, D. H.; Salter, D. A. *Polymer* **1967**, *8*, 139.
(4) McNeil, I. C.; Makhdumi, T. M. *Eur. Polym. J.* **1967**, *3*, 637.
(5) Cameron, G. G.; Kerr, G. P. *Eur. Polym. J.* **1970**, *6*, 423.
(6) Cameron, G. G.; Kerr, G. P. *Eur. Polym. J.* **1968**, *4*, 709.
(7) Grassie, N.; Melville, H. W. *Proc. R. Soc. London, A* **1949**, *199*, 14.
(8) Jellinek, H. H. G. *Degradation of Vinyl Polymers*; Academic: New York, 1955; p 74.
(9) MacCallum, J. R. *Makromol. Chem.* **1965**, *83*, 137.
(10) Brockhaus, V. A.; Jenckel, E. *Makromol. Chem.* **1956**, *18/19*, 262.
(11) McNeil, I. C. *Eur. Polym. J.* **1968**, *4*, 21.
(12) Cacioii, P.; Moad, G.; Rizzardo, E.; Serelis, A. K.; Solomon, D. H. *Polym. Bull. (Berlin)* **1984**, *11*, 325.
(13) Koz'mina, O. P.; Shirshova, A. N. *J. Appl. Chem. USSR (Engl. Transl.)* **1957**, *30*, 1952.
(14) Bresler, S. E.; Os'minskaia, A. T.; Popov, A. G.; Saminskii, E. M.; Frenkel, S. Ia. *Colloid J. USSR (Engl. Transl.)* **1958**, *20*, 381.
(15) Kashiwagi, T.; Hirata, T.; Brown, J. E. *Macromolecules* **1985**, *18*, 131.
(16) Hirata, T.; Kashiwagi, T.; Brown, J. E. *Macromolecules* **1985**, *18*, 1410.
(17) Hatada, K.; Kitayama, T.; Masuda, E. *Polym. J. (Tokyo)* **1986**, *18*, 395.
(18) Moad, G.; Solomon, D. H.; Johns, S. R.; Willing, R. I. *Macromolecules* **1984**, *17*, 1094.
(19) Hatada, K.; Kitayama, T.; Fujikawa, K.; Ohta, K.; Yuki, H. *ACS Symp. Ser.* **1981**, *166*, 327.
(20) Hatada, K.; Kitayama, T.; Okahata, S.; Yuki, H. *Polym. J. (Tokyo)* **1982**, *14*, 971.
(21) Busfield, W. K. In *Aspects of Degradation and Stabilization of Polymers*; Jellinek, H. H. G., Ed.; Elsevier Scientific: Amsterdam, 1978; p 62.
(22) Tsang, W., private communication.
(23) Bailey, W. J. *SPE Transaction*, **1965**, *5*, 1.
(24) to be published.
(25) Bevington, J. C. *Proc. R. Soc. London, A* **1951**, *231*, 420.
(26) Commercial equipment is identified in this paper in order to adequately specify the experimental procedure. Such identification does not imply that the equipment identified is necessarily the best available for the purpose.

Tri-*n*-butyltin Hydride Reduction of Poly(vinyl chloride): Kinetics of Dechlorination for 2,4-Dichloropentane and 2,4,6-Trichloroheptane

F. A. Jameison,[†] F. C. Schilling, and A. E. Tonelli*

AT&T Bell Laboratories, Murray Hill, New Jersey 07974. *Received March 5, 1986*

ABSTRACT: 2,4-Dichloropentane (DCP) and 2,4,6-trichloroheptane (TCH) were reductively dechlorinated with tri-*n*-butyltin hydride ($(n\text{-Bu})_3\text{SnH}$) directly in the NMR sample tube. Carbon-13 NMR spectra were recorded periodically to monitor the progress of DCP and TCH dechlorination. From these observations the following kinetic conclusions were drawn: (i) meso (*m*) DCP was reduced 30% faster than racemic (*r*) DCP; (ii) the Cl from DCP was removed 4 times faster than the Cl in 2-chloropentane or 2-chlorooctane; (iii) the 4-Cl in *mm*-TCH is removed faster than the 4-Cl in *mr*-TCH, which in turn is more reactive than the 4-Cl in the *rr* isomer; and (iv) the 4-Cl in TCH is removed 1.5 times faster than the 2- or 6-Cl's. Conclusions i and ii were previously observed at the diad level, at least qualitatively, in the $(n\text{-Bu})_3\text{SnH}$ reduction of poly(vinyl chloride) (PVC) to ethylene–vinyl chloride (E–V) copolymers. With the kinetic information obtained from the reduction of DCP and TCH, an attempt was made to simulate the $(n\text{-Bu})_3\text{SnH}$ reduction of PVC to E–V copolymers. Comparison of the structures of the E–V copolymers simulated on the computer with those determined for $(n\text{-Bu})_3\text{SnH}$-reduced PVC by ^{13}C NMR permits us to conclude that DCP and TCH are model compounds appropriate for studying the reductive dechlorination of PVC.

Introduction

Tri-*n*-butyltin hydride ($(n\text{-Bu})_3\text{SnH}$) has been used to reductively dechlorinate poly(vinyl chloride) (PVC) to polyethylene (PE) during the course of studying the microstructure of PVC.[1] The structure of the starting PVC is deduced from that of the PE resulting from its complete dechlorination. Partial reduction of PVC with $(n\text{-Bu})_3\text{SnH}$ has also produced a series of ethylene–vinyl chloride (E–V) copolymers. ^{13}C NMR analysis of these E–V copolymers has revealed the details of their microstructures.[2]

This series of E–V copolymers, which is not possible to obtain either by copolymerization of E and V monomers or by chlorinating PE, was found to have the same chain length as the starting PVC. As the amount of Cl removed was increased, it was observed that the ratio of racemic

---

[†] Current address: State University of New York at Stony Brook.